



## MODELLING RIM IMPACT AND ULTIMATE BEHAVIOUR OF TRIPLE FRICTION PENDULUM BEARINGS

P. Tomek<sup>(1)</sup>, H. Darama<sup>(2)</sup>, R. Sturt<sup>(3)</sup> and Y. Huang<sup>(4)</sup>

<sup>(1)</sup> Senior Engineer, Arup, [pavel.tomek@arup.com](mailto:pavel.tomek@arup.com)

<sup>(2)</sup> Associate, Arup, [huseyin.darama@arup.com](mailto:huseyin.darama@arup.com)

<sup>(3)</sup> Director and Arup Fellow, Arup, [richard.sturt@arup.com](mailto:richard.sturt@arup.com)

<sup>(4)</sup> Senior Analyst, Arup

### **Abstract**

Triple Friction Pendulum (TFP) bearings are widely used for base isolation applications in North America and other high seismic regions. However, their factor of safety at rim impact and the ultimate behavior has not been well studied. ASCE 7 requires isolator displacement capacity dimensions to be calculated from average MCE displacement demands. By definition it means that some of the earthquakes will be higher. Individual ground motion analyses may predict displacements exceeding isolator capacity by factor of 2 or more. This will lead to rim impact, increased superstructure demands and reduced stability of isolators/structure that are not accounted for. For sites with near field pulse-like motions excessive displacements and chances of rim impact further increase. An accurate model capturing the ultimate isolator forces and displacements is therefore crucial for determination of superstructure demands and stability in both performance-based design of new buildings and evaluation of existing buildings. However, until now there was no design guidance or commercial software available that would capture this behavior.

In this study, the authors performed a series of parametric analyses using nonlinear finite element models of TFP isolators to understand the behavior of bearings subjected to rim impact. The models contained detailed geometry, sliding contact between components, and material behavior including the potential for loss of stability. The effect of axial force was studied to quantify the effect on the isolator lateral resistance. One of the conclusions of the study was that although the lateral force in the TFP bearings is proportional to the axial force, the ultimate capacity of an isolator rim is constant for an isolator type.

The understanding gained from the study served as a basis for implementation of a simplified rim impact and failure model into an existing seismic isolator model in LS-DYNA in which the behaviors of a sliding bearing are encapsulated in a single element suitable for inclusion in models of whole buildings. The improved model was validated against results of physical testing of a full-scale TFP isolator and demonstrated satisfactory agreement. Thanks to the improvements, global as well as local effects of isolator impact can be captured in non-linear response history analysis (NLRHA) of buildings and quantified in terms of base shear, drift, member forces, etc.

This paper will summarize past research and literature on the subject, present the findings of the parametric FEA study, describe the features implemented into LS-DYNA including their validation against the physical test and conclude with general recommendations for the design and analysis of TFP bearings with rim impact in NLTHA.

*Keywords: Seismic Isolation, Performance Based Design, LS-DYNA, Time History Analysis, Impact*



## 1. Introduction

Triple Friction Pendulum (TFP) bearings are widely used for base isolation applications in North America and other high seismic regions as an effective earthquake protection system. TFP bearings increase the building's period and damping and as a result reduce the superstructure seismic demands. The demand reduction comes at the expense of large relative displacements concentrated at the isolation level. Design displacement demands and requirements for isolator dimensions are well defined in various national codes. ASCE 7 for example requires in Section 17.5.3.1 isolator dimensions to be calculated from average Maximum Considered Earthquake (MCE) displacement demands  $D_M$  [1]. However, the behavior and requirements for the isolators in extreme events exceeding design displacements are not very well defined and understood.

To achieve the basic code objective of Life Safety (Collapse Prevention) it is important that isolated structures satisfy the ASCE 7 stipulated Target Reliability for Structural Stability. Therefore, both the structure and the isolators require factors of safety. Since the structural component material standards for concrete, steel, etc. have these safety factors in their respective standards (ASTM, AISC, ACI, etc.) it is assumed and proven by earthquake performance that the Target Reliability for Structural Stability is satisfied. However, for isolators because of lack of such equivalent standards it is important to evaluate the shear and displacement factors of safety of isolators to satisfy the ASCE 7 Target Reliability of Structural Stability [2,3,4].

When Non-Linear Response History Analysis (NLRHA) is used in design or when higher than code required hazard is considered in seismic assessment, some ground motions may exceed  $D_M$  by factor of 2 or more [4] which can result in impact either onto the rim of the isolator or the moat wall. For sites with near field pulse-like motions excessive displacements and chances of impact further increase. Impact results in increased superstructure demands and higher probability of collapse. While several publications focus on the moat impact [5,6,7], impact onto the isolator rim and ultimate behavior of isolator has not been well studied.

An accurate model capturing the ultimate isolator forces and displacements is crucial for determination of superstructure demands in both performance based design of new buildings and evaluation of existing buildings. To gain a better understanding of the behavior of bearings subjected to rim impact, the authors performed a series of parametric analyses using nonlinear finite element models of TFP isolators. The models contained detailed geometry, sliding contact between components, and material behavior including the potential for loss of stability. The effect of axial force was studied to quantify the effect on the isolator lateral resistance.

This paper will summarize past research and literature on the subject, present the findings of the parametric FEA study, describe the features implemented into LS-DYNA including their validation against a physical test and conclude with general recommendations for the design and analysis of TFP bearings with rim impact in NLRHA.

### 1.1 Isolator regimes

The design of the rim in friction pendulum bearings varies by region (see Fig. 1). In the United States, the pendulum bearings typically have a rim cast with the body of the isolator. In Japan, the rim is generally bolted to the body of the isolator and therefore has a lower strength and factor of safety against isolator failure. In Europe, the retaining rim is not allowed in the code. This paper focuses on the US practice; however, its conclusions and recommendations can be applied for other designs as well.

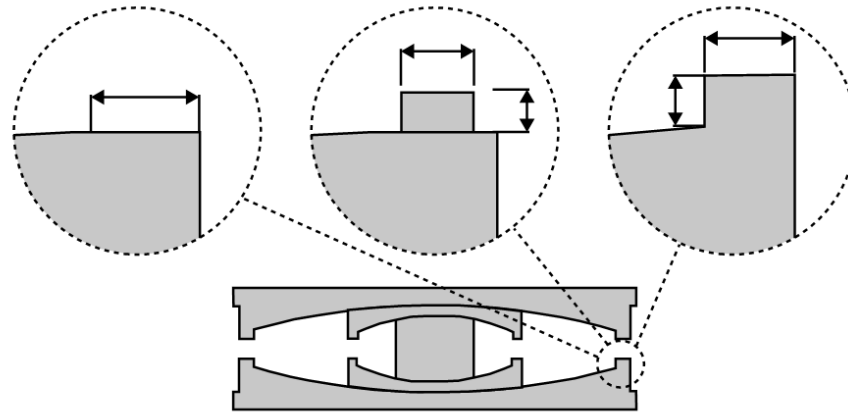


Fig. 1 – Different design considerations for isolator rims – Europe, Japan, and US

The TFP bearing has transitions in stiffness and damping resulting from the various combinations of sliding that occur on the multiple concave surfaces. As described in Fenz & Constantinou [8], a triple pendulum bearing has 5 regimes (see Fig. 2 and Fig. 3). During Regime V all components of the isolator are in contact, components start deforming elastically and the following regimes can be described as:

- Regime VI – the capacity of one of the rims is reached (typically the outer rim) and the rims start yielding,
- Regime VII – the inner slider moves far enough over the rim that the isolator loses stability to support vertical and lateral loads.

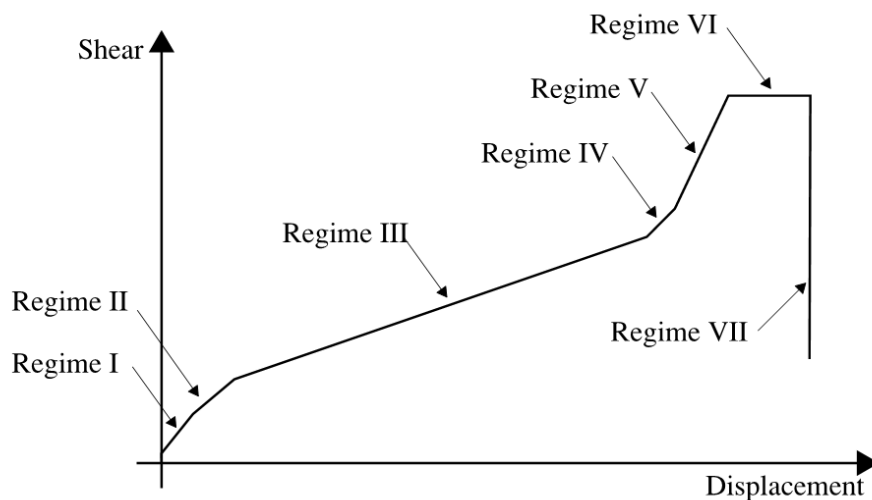


Fig. 2 – Theoretical Force-Displacement curve of for a typical TFP isolator

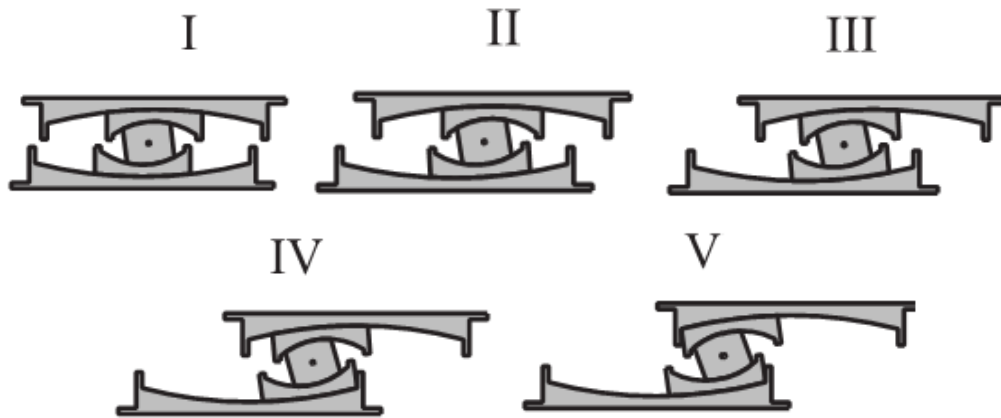


Fig. 3 – Triple friction pendulum bearing displacement regimes [8]

### 1.2 Isolator modeling in NLRHA

In NLRHA the variation in ground motions results in some time history scenarios exceeding average design displacements and reaching Regimes IV, V, VI and VII. The overall structural response is then dependent on the accuracy of the modelling of those regimes. Fig. 4 demonstrates the effect of the different rim modelling on the individual and averaged response. If the rim is not modelled (Case A, which is the typical practice) base shears and associated superstructure member demands can be underestimated while the isolator displacements may be overestimated. On the other hand, if the rim impact is modelled as rigid or stiff without a strength limit (Case C) base shears can be overestimated while isolator displacements can be underestimated. This is true for both the individual ground motions as well as the average (mean) values which are typically used for design. To accurately capture the superstructure demands and isolator displacement both impact and ultimate capacity should be considered (Case B).

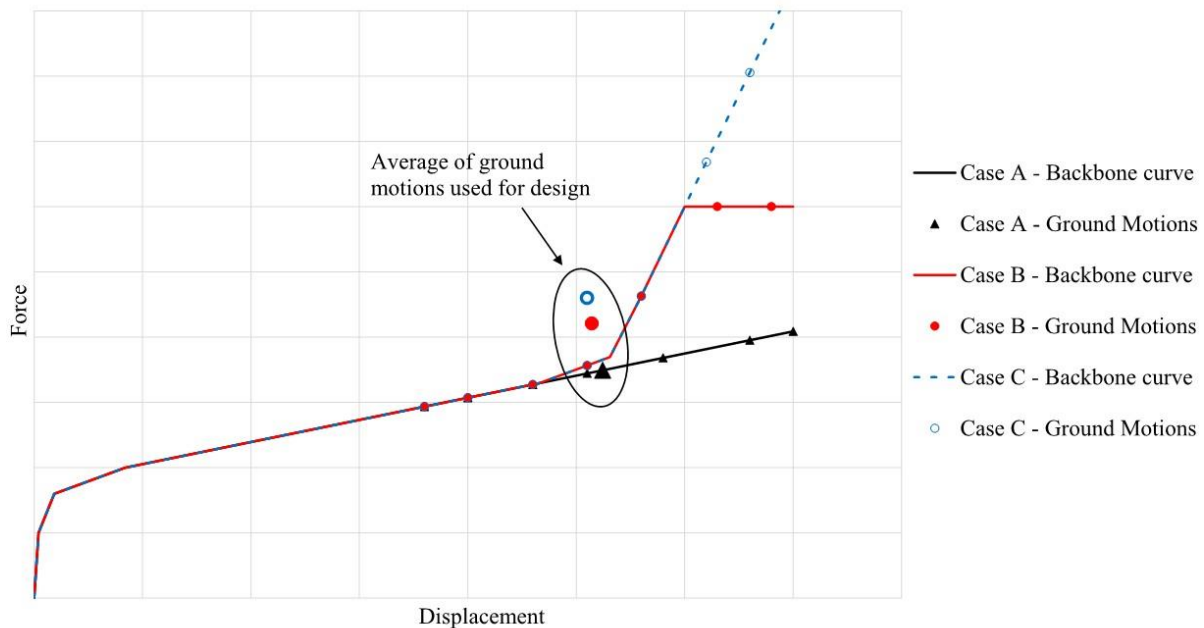


Fig. 4 – Effect of rim modelling on average design demands in NLRHA



### 1.3 Past research of isolator impact

Kitayama & Constantinou [5] demonstrated that isolator rim impact (and other displacement restraints) may result in increases in probability of collapse of certain isolated buildings and recommended reassessment of ASCE 7 criteria. It also highlighted that if the isolators do not have the necessary factor of safety for displacement and shear, it could lead to a catastrophic collapse situation for structure/isolator [2]. To achieve acceptable probability of collapse the isolator displacement capacity and location of the moat wall should be increased compared to the code required  $D_M$ . The increase depends on the superstructure type, type of restraint and risk category. Flexible structures (e.g. moment frames) are less affected while stiff structures (e.g. braced frames) will require more significant increase in displacement capacity.

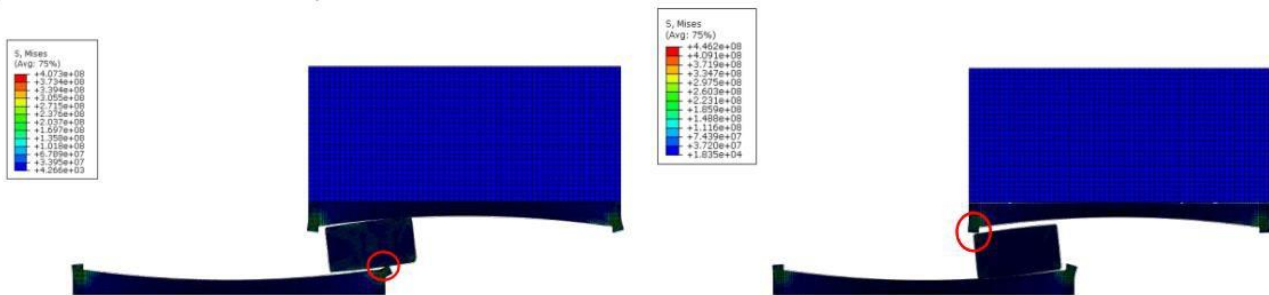


Fig. 5 – Two failure mechanisms of pendulum bearings – uplift (right) and rim yielding (left) [9]

The ultimate capacity and failure mechanisms of different isolator rims of double pendulum bearings was studied by Bao & Becker [9,10,11]. Firstly, Bao & Becker performed a series of analyses focused on the failure modes under pulse like motions [9,10]. Two modes of failure were observed in the tests depending on the axial force in the isolators (see Fig. 5). Isolators with low slider pressures failed in uplift (10MPa/1.45ksi) while isolators with high slider pressure failed in rim yielding (50MPa/7.25ksi).

Secondly [11], the researchers tested double pendulum isolators with various rim types (see Fig. 1). The tested isolators were scaled down models by length factor  $L=3.5$  and tested with a concrete block on top resulting in a slider pressure of 21.5 MPa (3.1 ksi). The capacities of isolators with different rim designs ranged from 37 kN (8.4 kip) to 92 kN (20.7 kip). Equivalent full-scale capacity of the isolator most resembling to the US isolator type (Specimen C) can be estimated as  $3.5^2 \times 16.6 \text{kip} = 205 \text{kip}$  (converted to full scale isolator).



Fig. 6 – Full scale TFP isolator after ultimate capacity test



#### 1.4 Full scale isolator tests

Over the years Arup gathered data from various projects using TFP isolators that performed project specific ultimate capacity tests in addition to isolator tests required by ASCE 7 (see Fig. 6). Table 1 and Fig. 7 shows the results of ultimate capacity tests of isolators from four projects – all US type with a rim cast with the body of the isolator. The maximum total shear from the tests varies with axial force with values ranging from 510 kip to 1071 kip. The “Rim only” shear capacity, defined as the lateral force relative to the isolator lateral force at the end of Regime IV, ranges from 196 kip to 394 kip. It is important to note that in Regime V and VI the isolator sliders are still resisting the lateral forces and act in parallel with the rim resistance force, therefore “Rim only” strength is a better comparison between the tests as each test had a different axial force and friction parameters and therefore different isolator response.

Table 1 – Summary of isolator capacities from isolator tests on select Arup projects

Project	Axial Force	Outer Slider Pressure	Total Shear Capacity	Rim Only Shear Capacity
Project A	1695 kip	2.4 ksi	717 kip	395 kip
Project B	2731 kip	5.1 ksi	719 kip	315 kip
Project C	3056 kip	3.8 ksi	1071 kip	337 kip
Project D	1250 kip	3.3 ksi	510 kip*	196 kip*

\*Isolator did not reach its full capacity before the test stopped

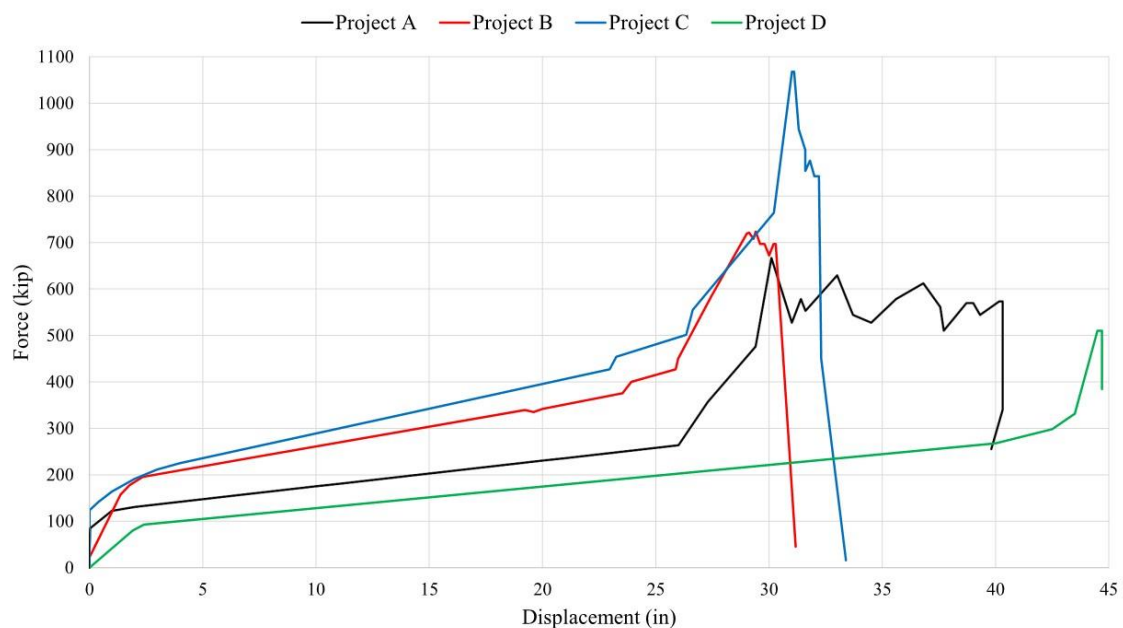


Fig. 7 – Force-displacement plot of ultimate capacity tests of TFP isolators from various Arup projects



## 2. Parametric FEA studies

To understand the behavior of triple pendulum bearings, a series of FEA analyses in LS-DYNA with explicitly modeled isolators with rims was performed. The isolator model (see Fig. 8) consists of the sliders modeled with rigid shells, contact surfaces between the components, and a partial rim modeled with elastic-plastic solid elements. The friction between the sliding surfaces was set to  $\mu_1 = 0.07$ ,  $\mu_2 = \mu_3 = 0.02$ ,  $\mu_4 = 0.07$ .

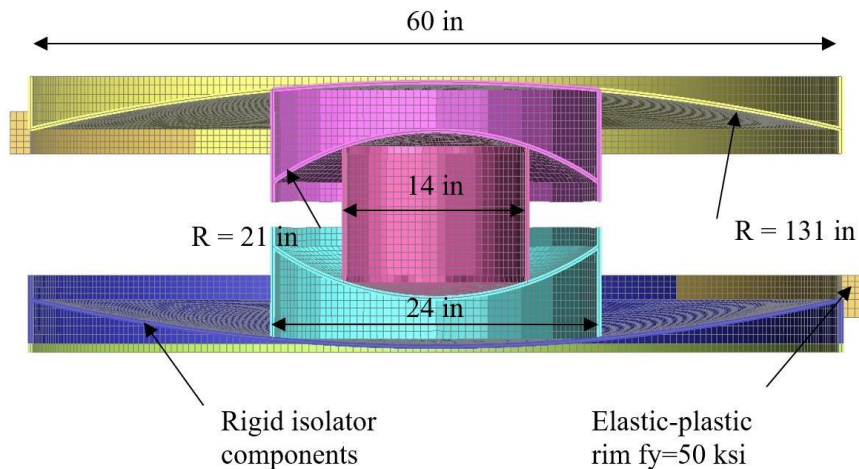


Fig. 8 – FEA model of TFP isolator with elastic-plastic rim

### 2.1 Rim impact behavior under different slider pressures

The first set of analyses concentrated on the effect of slider pressure on the rim impact behavior. The model was loaded with different masses above the isolator resulting in outer slider pressures ranging from 1.0 to 12.0 ksi. A monotonically increasing displacement with velocity approx. 30in/sec was imposed to the top isolator slider.

The results showed the two failure modes described by Bao & Becker [9,10] – i.e. uplift/overturning with small downward pressure and rim yielding with large downward pressure (see Fig. 9, Fig. 10). The threshold between the two modes depends on the rim strength and isolator geometry. In this study the transition from uplift to rim yielding was observed at approx. 3 ksi.

In most projects the isolators are designed to more than 3 ksi pressure (see Table 1), therefore the dominant failure mode for typical buildings is rim yielding.

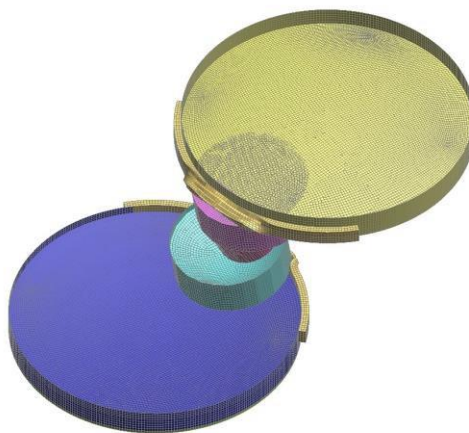


Fig. 9 – Deformation of rim at failure stage with rim yielding

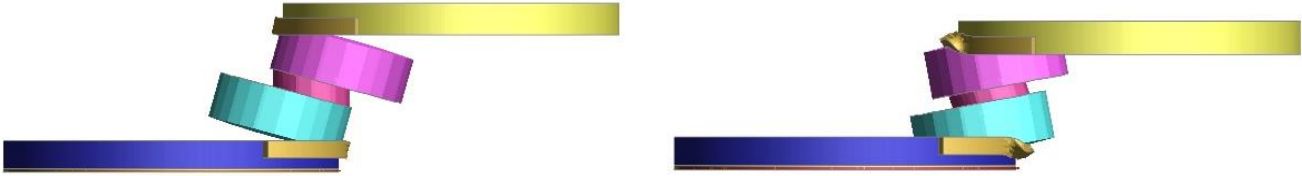


Fig. 10 – Two modes of TFP isolator behavior at ultimate displacement depending on axial force – uplift/overturning (left) and rim yielding (right)

## 2.2 Effect of axial force on isolator strength

A significant modeling and design parameter that has not been widely studied and addressed in past research papers is the lateral capacity of isolators after impact and its variability with axial force in the isolators.

In friction pendulum bearings the lateral force is directly proportional to the axial force. In this study it is also investigated whether the ultimate capacity is also directly proportional to the axial force or a constant value.

Fig. 11 shows the force displacement plots of the models with various slider pressures described above. Before impact the model follows the backbone curve. After impact the force increases and then the rim starts yielding and locally failing (or uplifting for low slider pressures). The shear response after impact is fluctuating – this is due to relatively coarse mesh of the model, use of rigid elements for some parts of the model and inner vibration that causes instantaneous changes in axial force. Despite relatively crude results some conclusions can already be drawn if the ultimate capacity of the isolator is taken as an average.

Fig. 12 shows the development of shear capacity of the model depending on the axial force. For increasing axial load, the total shear capacity increases. However, the “rim only” strength (the shear force relative to the end of Stage IV) is approximately constant across varying levels of axial load. This suggests that the lateral force at the rim failure is a combination of the lateral force in the contact surfaces between the isolator components and the rim only yield capacity. The former is dependent on the axial force while the latter is constant:

$$V_{u,tot}(W) = V_{slider}(W) + V_{y,rim} \quad (1)$$

The first value,  $V_{slider}(W)$ , can be calculated based on isolator properties (radii and friction values) and was previously described by Fenz, & Constantinou [8] and varies with instantaneous axial force on the isolator ( $W$ ). The second value  $V_{y,rim}$  (i.e. capacity of the rim itself) is a fixed value that may be based on isolator manufacturer’s recommendations, tests (Section 1.4) or analysis. This analysis predicts rim capacity 638kip (rim thickness = 1.5”, rim height = 2”, steel  $f_y = 50$ ksi).

Further parametric studies are needed to establish guidance for the rim capacity. The authors believe that the main parameters impacting the rim strength are rim thickness, steel strength of the casting and size of the inner and outer isolator components.



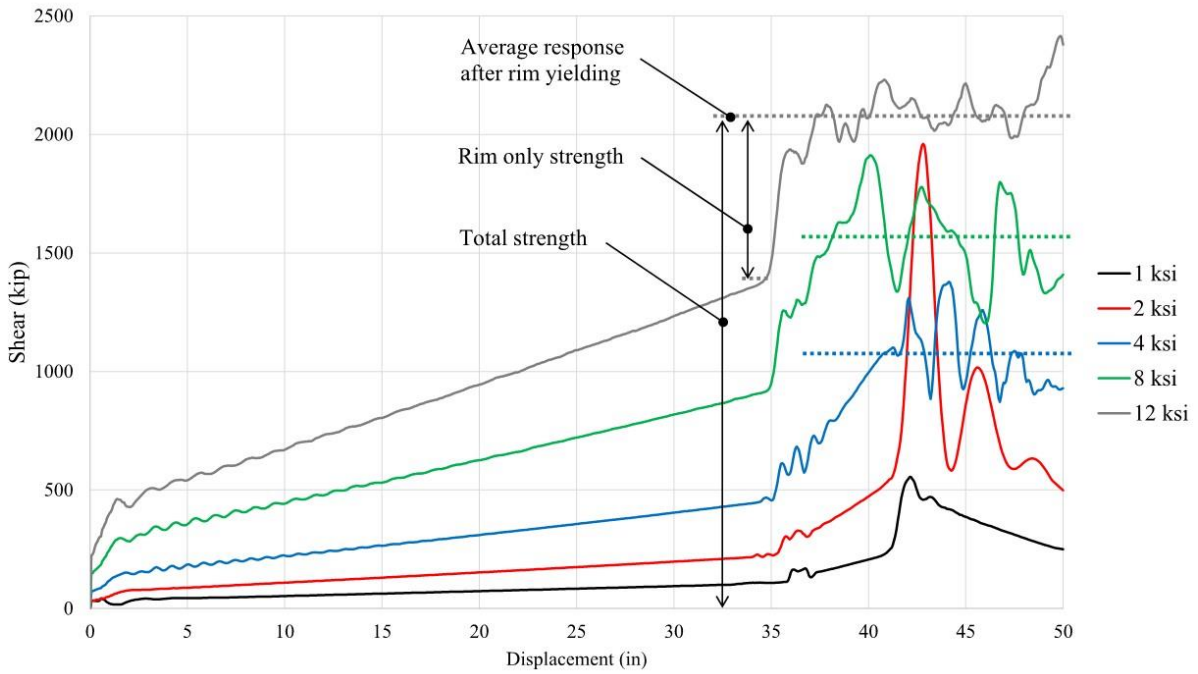


Fig. 11 – Force-displacement chart – result of analysis with various axial forces

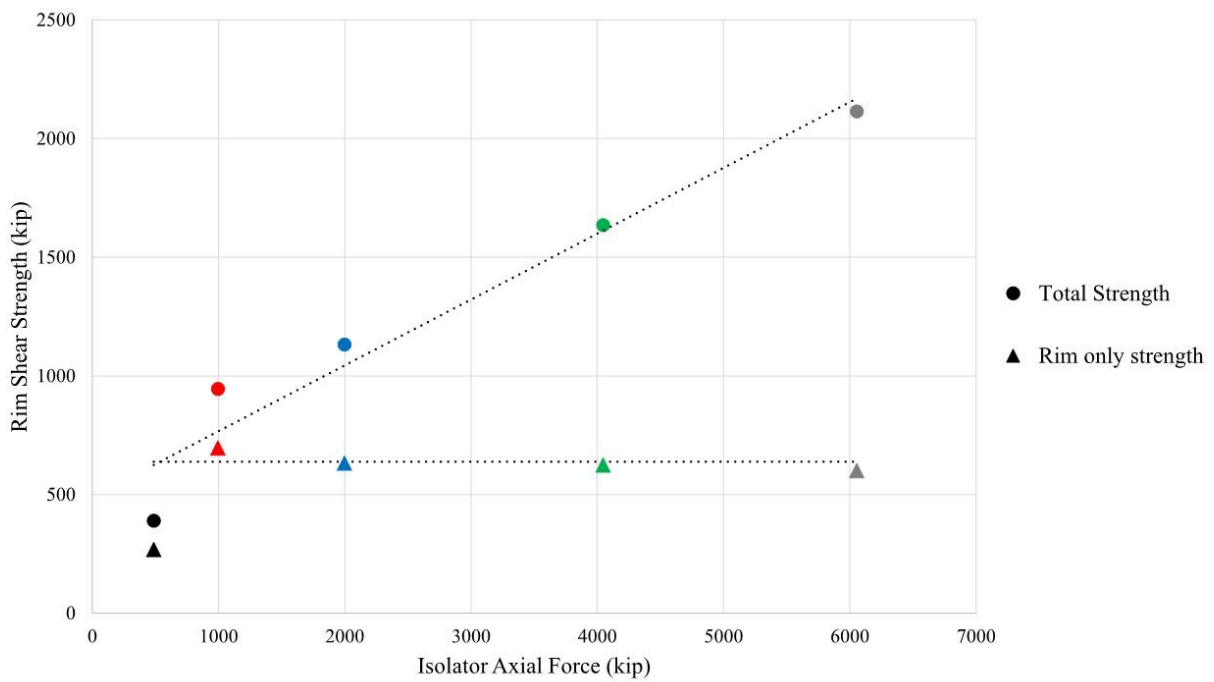


Fig. 12 – Comparison of the absolute rim capacity at various axial forces



### 3. Simplified material model for isolators in LS-DYNA

MAT\_197: SEISMIC\_ISOLATOR is a material model in LS-DYNA capturing the behavior of TFP bearings in NLRHA. The five phases of a TFP bearing are modelled with three elements in series, each representing a single concave friction pendulum with properties according to the model developed by Fenz & Constantinou [8]. See LS-DYNA Keyword User's Manual for further details [12].

Previously MAT\_197 included a stiff rim defined by its distance from center and stiffness. As part of this study the authors updated the material model to include a rim yielding and failure (phases VI and VII). This option, which will be available in future releases of LS-DYNA, requires two new input parameters:

FYRIM Radial force at failure of rim ("rim only" yield strength, rather than the yield force for the whole device)

DFRIM Radial displacement of rim to failure defined as the total radial displacement including the ring size and elastic ring deformation. The element is deleted from the analysis once the DFAIL displacement is reached.

Rim deformation is modelled using a classical plasticity approach with damage and failure. Regarding the distribution of damage around the rim circumference, plastic deformation is tracked such that repeated impacts at the same point result in cumulative damage. However, impact at a point separated by more than 45 degrees around the rim from the previous impact is treated as a new impact, and damage then starts from zero.

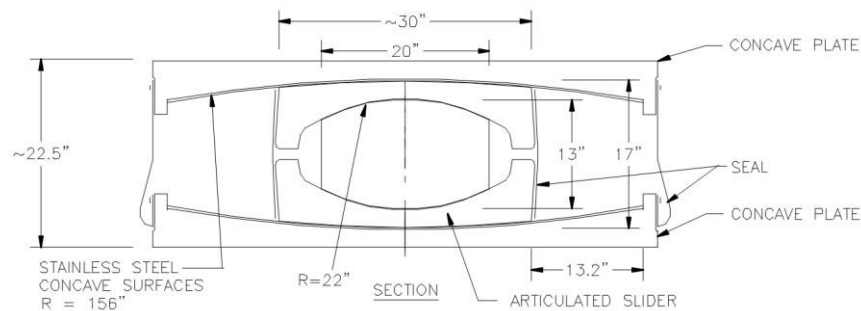


Fig. 13 – Geometry of the tested isolator

#### 3.1 Validation of the simplified model against physical testing

To validate the simplified model with three elements in series, it was tested against results of physical testing from Project A (see Table 1). The isolator properties were based on the isolator geometry (Fig. 13) and friction values measured in the physical test:  $\mu_1 = 0.072$ ,  $\mu_2 = \mu_3 = 0.047$ ,  $\mu_4 = 0.085$ . The rim capacity FYRIM was taken from the tests as 395 kip and set for the upper and lower elements in the series model. The middle element was modelled with standard setting with stiff rim without failure. The stiffness of the rim STIFFL for all three elements was estimated as 600 kip/in. The isolator model was subjected to a full displacement reversal to 40" and -40" with axial force matching the test (1696kip, see Table 1).

The resulting force-displacement curve (see Fig. 14) matches very well with the response of the isolators from physical tests including the force reversal and resistance of the rim opposite the initial impact. The softening after the rim yielding does not perfectly follow the physical results – it drops too quickly. It is noted as a future improvement to the material model.

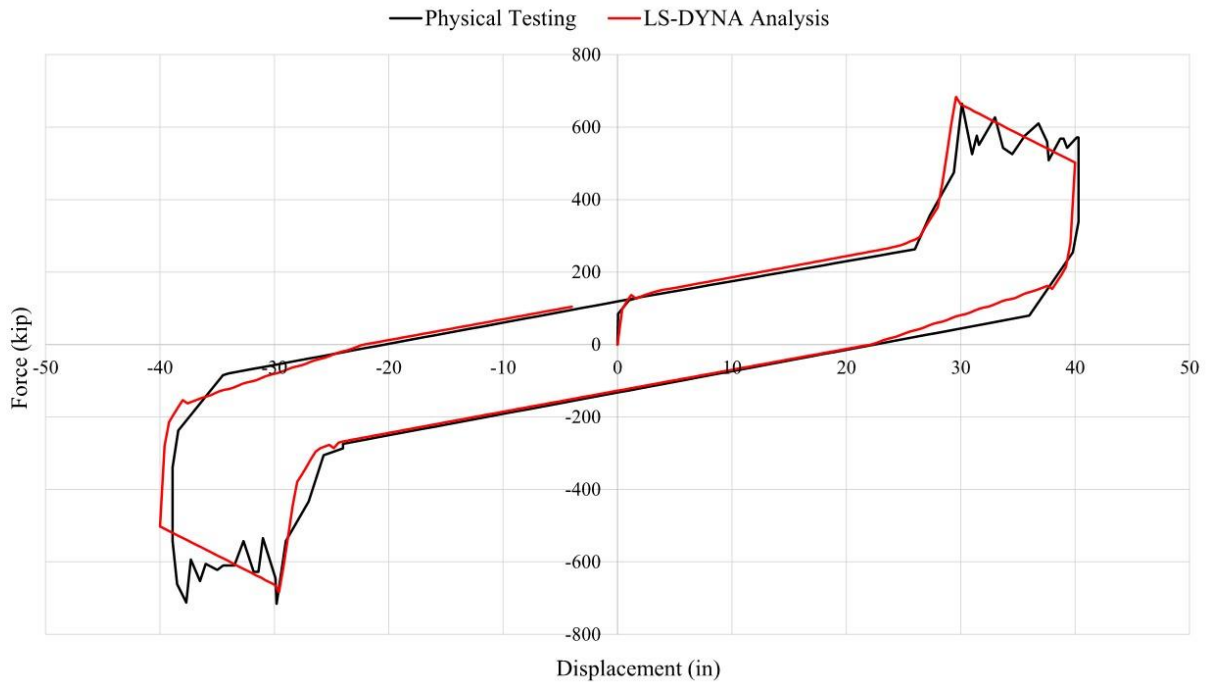


Fig. 15 – Comparison of physical tests (Project A) with simplified LS-DYNA modeling

#### 4. Conclusion

This paper describes the importance of consideration of impact and ultimate capacity of TFP bearings in the design of isolated buildings. ASCE 7 requires isolator dimensions to be calculated from average MCE displacement demands, but individual ground motion in NLRHA may predict displacements exceeding isolator displacement capacity leading to rim impact and increased superstructure demands.

The authors reviewed past research and physical tests and performed a series of analyses using nonlinear finite element models of TFP isolators to understand the behavior of bearings subjected to rim impact. The models contained detailed geometry, sliding contact between components, and material behavior including the potential for failure.

The understanding gained from the parametric study served as a basis for implementation of a simplified rim impact and failure model into an existing seismic isolator model in LS-DYNA in which the behaviors of a sliding bearing are encapsulated in a single element suitable for inclusion in models of whole buildings. The improved model was validated against results of physical testing of a full-scale TFP isolator and demonstrated satisfactory agreement.

In the design of new buildings, it is recommended to increase isolator displacement and shear capacity based on Kitayama & Constantinou [5] to avoid increased probability of collapse in extreme events. For existing buildings or isolators with code based minimum dimensions LS-DYNA offers a material model for NLRHA capturing the impact and yielding of the isolator rim that allows accurate assessment of superstructure demands and isolator displacements in models of whole buildings.

At the time of this research work, a novel concept of providing increased shear capacity is being implemented in the new TFP design. This development has been a result of satisfying the minimum factor of safety in the isolator displacement and shear capacity specified in the Seismic Isolation Standard for Continued Functionality [13] for satisfying the ASCE 7 Target Reliability for Structural Stability.



## 5. Acknowledgements

The authors would like to thank Arup for funding for this internal research and LS-DYNA developers for implementation of the material model into the source code. Also, we would like to acknowledge Simon Rees, Murat Melek, Gregory Nielsen, Lauren Biscombe and Alireza Sarebanha (all Arup) for their suggestions, comments and reviews of the study.

## 6. References

- [1] ASCE (2016): Minimum Design Loads for Buildings and Other Structures (ASCE 7-16), *American Society of Civil Engineers*, Reston, Virginia, USA.
- [2] Kitayama S, Constantinou M. (2018): Seismic Performance Assessment of Seismically Isolated Buildings Designed by the Procedures of ASCE/SEI 7, *MCEER 18-0004*, Multidisciplinary Center for Earthquake Engineering Research, Buffalo, NY, USA.
- [3] Shao B., Mahin S., Zayas V. (2017): *Member Capacity Factors for Seismic Isolators as Required to Limit Isolated Structure Collapse Risks to Within ASCE 7 Stipulated Structure Collapse Risk Limits*, University of California Berkeley, California, USA.
- [4] Zayas V., Mahin S., Constantinou M. (2016): *Safe and Unsafe Seismically Isolated Structures*, Pacific Earthquake Engineering Research Center, Berkeley, California, USA.
- [5] Kitayama, S., Constantinou, M. (2018): Effect of displacement restraint on the collapse performance of seismically isolated buildings. *Bulletin of Earthquake Engineering*, 17: 2767.
- [6] Masroor A, Mosqueda G (2015) Assessing the collapse probability of base-isolated buildings considering pounding to moat walls using the FEMA P695 methodology. *Earthquake Spectra*, 31(4), 2069–2086.
- [7] Sarebanha A., Mosqueda G., Kim M.K., Kim J.H. (2018): *Seismic response of base isolated nuclear power plants considering impact to moat walls*. Nuclear Engineering and Design, 328, 58-72.
- [8] Fenz DM and Constantinou MC (2008): Modeling triple friction pendulum for response history analysis, *Earthquake Spectra*, 24, 1011-1028.
- [9] Bao Y., Becker T. C. (2016): Predicting failure in sliding isolation bearings under long-period motion, *CSCE5th International structural specialty conference*. London, Ontario, Canada, June 1–4 2016.
- [10] Bao Y., Becker T. C., Hamaguchi H., (2017): Failure of double friction pendulum bearings under pulse-type motions, *Earthquake Engineering & Structural Dynamics*, 46, 715-732.
- [11] Bao Y., Becker T. C., Sone T., Hamaguchi H., (2017): Experimental study of the effect of restraining rim design on the extreme behavior of pendulum sliding bearings, *Earthquake Engineering & Structural Dynamics*, 47 (4).
- [12] LS-DYNA Keyword User's Manual – Volume II – Version R11 (2019), *Livermore Software Technology Corporation (LSTC)*, Livermore, CA 94551, USA
- [13] Zayas V., Mahin S., Constantinou M. (2017), *Seismic Isolation Standard for Continued Functionality*, Earthquake Protection Systems, Vallejo California, California, USA.